

MULTI-ORGAN AUTOMATIC SEGMENTATION IN 4D CONTRAST-ENHANCED ABDOMINAL CT

Marius George Linguraru and Ronald M. Summers

Diagnostic Radiology Department, Clinical Center, National Institutes of Health, Bethesda MD, USA
lingurarum@mail.nih.gov

ABSTRACT

Medical imaging and computer-aided diagnosis (CAD) traditionally focus on organ- or disease-based applications. To shift from organ-based to organism-based approaches, CAD needs to replicate the work of radiologists and analyze consecutively multiple organs. A fully automatic method is presented for the simultaneous segmentation of four abdominal organs from 4D CT data. Abdominal contrast-enhanced CT scans from sixteen patients were obtained at three phases: non-contrast, arterial and portal. Intra-patient data is registered non-rigidly using the demons algorithm and smoothed with anisotropic diffusion. Mutual information accounts for intensity variability within the same organ during subsequent acquisitions and data are interpolated with cubic B-splines. Then heterogeneous erosion is applied to multi-phase data using the intensity characteristics of the liver, spleen, and kidneys. The erosion filter is a 4D convolution that preserves only image regions that satisfy the above intensity criteria. Finally, a geodesic level set completes the segmentation of the four abdominal organs. This 3D evaluation of abdominal data shows great promise as a computer-aided radiology tool for multi-organ and multi-disease analysis.

INDEX TERMS: Abdominal imaging, liver, spleen, kidneys, segmentation, registration, contrast-enhanced CT.

1. INTRODUCTION

Medical imaging and computer-aided diagnosis traditionally focus on organ- or disease-based applications. Very little work has been presented toward the automatic simultaneous detection and segmentation of multiple organs or different types of abnormalities.

Chronologically, Gao et al. proposed a 3D deformable surface model to segment the kidneys in CT [2]. They initialize the model manually and discuss its potential to segment other abdominal organs. Park et al. use a database of 32 hand-segmented CT abdominal scans to compute a mean image [5]. This is registered with thin plate splines to

propagate the segmentation of liver, kidneys and aorta. Using a similar principle, a priori data from probabilistic atlases is used to initialize the segmentation of abdominal organs in [9] and [11]. Both methods use measures of relationship and hierarchy between organs and manual landmarks. Finally, multi-dimensional CT data from four-phases are employed in [3,7]. Hu et al. [3] use independent component analysis in a variational Bayesian mixture, while Sakashita et al. [7] combine expectation-maximization and principal component analysis to segment abdominal CT.

Our method is fully automatic, image intensity-based and does not use any a priori probabilistic information on shape or location. We use fewer CT phases than alternative work and propose a 4D convolution to detect abdominal organs, followed by a refinement of the segmentation by geodesic active contours.

2. METHOD

An example of multi-phase CT is presented in Figure 1. Although the acquisitions are done during the same session and intra-patient, note the abdominal motion especially at the liver, spleen and right kidney. Images from three phases of contrast-enhanced abdominal CT data (non-contrast, arterial and portal phases) are registered. Since data are acquired during a single acquisition session, inter-acquisition motion is mainly due to breathing and cardiac pulsation, though small patient movements are also present. To account for motion artefacts, non-contrast and arterial phases are registered to the portal phase. A comparison between rigid, affine and non-rigid registration algorithms for intra-patient abdominal CT images is further performed. Data are interpolated with cubic B-splines.

The demons non-rigid registration algorithm is employed, as the limited range of motion ensures partial overlaps between each organ over multiple phases [10]. The deformation field D of image I to match image J is governed by the optical flow equation and can be written as [10]

$$D = \frac{(I - J)\nabla J}{\|\nabla J\|^2 + (I - J)^2};$$



Figure 1: Multi-phase abdominal 4D CT data. 2D slices of 3D volumes: (a) non-contrast, (b) arterial phase and (c) portal phase data. For visualization purposes, 3D volumes are aligned according to the position in the scanner.

The multi-phase CT data is intra-modal, but the different levels of organ enhancement justify the use of a multimodal similarity measure. Mutual information m accounts for intensity variability within the same organ during multi-phase acquisitions, where $p(i,j)$ is the joint probability distribution of images I and J , and $p(i)$ and $p(j)$ the marginal distributions [4].

$$m(I | J) = \sum_{i,j} p(i, j) \log \frac{p(i, j)}{p(i)p(j)} ;$$

Registered data are smoothed using anisotropic diffusion to enhance the homogeneity of each abdominal organ and ensure boundary preservation. We employ the classic Perona-Malik anisotropy model [6].

Given the smoothed data, intensity characteristics of four organs are extracted from a random 4D dataset, after verifying that the time series enhanced according to the acquisition phase. This analysis is required only once and is independent of the algorithm flow. It estimates a set of minimum and maximum 3D intensities for the four categories of organs to segment at each level of enhancement: $min_{p,r}$ and $max_{p,r}$, where $p=1..3$ for liver, spleen and kidney (assuming the left and right kidney share the same range of intensities), and $r=1..3$ for pre-contrast, arterial and venous phases.

The intensity characteristics imbedded in $min_{p,r}$ and $max_{p,r}$ were input to an erosion filter that is applied to multi-phase data. A 4D array $K(x,y,z,t)=I_t(x,y,z)$ is created from the multi-phase data, where $t=1..3$ for pre-contrast, arterial and venous phases. The heterogeneous erosion was implemented as a convolution with a 4D filter f that preserved and labeled only regions for which all their voxels satisfy the intensity criteria (given the erosion element). S represents the labeled image and l_q the labels ($q=1..4$ for liver, spleen, left kidney and right kidney).

$$S(x, y, z) = (K \circ f)(x, y, z, t) = \begin{cases} l_q, & \text{if } \bigcap_t (\min_{qt} \leq K(x, y, z, t) \leq \max_{qt}) ; \\ 0, & \text{otherwise} \end{cases}$$

All the considered organs have similar Hounsfield units (HU) before enhancement; hence the processing burden of the 4D filter is reduced by including data from only two phases: arterial and portal. This allows eliminating the blood vessels and the heart, some of the major sources of error for liver segmentation. Connected component analysis of labeled data facilitates reducing additional false positives. Thresholding in the non-contrast data corrects for residual errors from the stomach, while the spine is eliminated for its high standard deviation and lack of enhancement between phases.

Finally, the labeled data are used as input level image (zero-level) L_0 into a geodesic active contour L [1]. The venous phase CT scan (I_3) provides the feature image, while the sigmoid of the gradient of I_3 supplies an edge image I_e , with α and β computed from ∇I_3 . The weights w_1 , w_2 and w_3 control respectively the speed c , curvature k and attraction to edges [1].

$$I_e = 1 - 1 / (1 + \exp(-(\nabla I_3 - \alpha) / \beta));$$

$$\frac{dL}{dt} = I_e (w_1 c + w_2 k) |\nabla L| + w_3 \nabla I_e \nabla L ;$$

The segmented organs have their margins eroded as a result of the convolution with the 4D filter. Unlike a typical morphological dilation, the active contour accounts for the eroded margins of the segmented organs using intensity, edge and curvature information. Moreover, the intensity and edge information input into the geodesic active contour provides accurate data to correct for the possible bias in the estimation of the intensity characteristics $min_{p,r}$ and $max_{p,r}$.

3. RESULTS

The 16 studies had three temporal 3D acquisitions. The first image is obtained before contrast. Then the patients are injected with 130ml of ISOVUE-300 and two more contrast-enhanced data acquisitions are completed during arterial and portal phases. The distinction between phases was performed using fixed-delays. No patients had any of the four organs (liver, spleen, left and right kidney) or parts of them removed, though abdominal abnormalities were present in all cases. The CT data were collected using GE LightSpeed Ultra and GE LightSpeed QX/I scanners (GE Healthcare). Image resolution ranged from $0.62 \times 0.62 \times 5.0 \text{ mm}^3$ to $0.82 \times 0.82 \times 5.00 \text{ mm}^3$. Image size ranged from $512 \times 512 \times 41 \text{ voxels}^3$ to $512 \times 512 \times 147 \text{ voxels}^3$.

The implementation uses Visual C++ 8.0 (Microsoft), OpenGL (SGI) and the Insight Segmentation and Registration Toolkit (ITK) 2.4 (Kitware, Inc.). 3D rendering and visualization of the segmentation was generated using VolView (Kitware, Inc.)

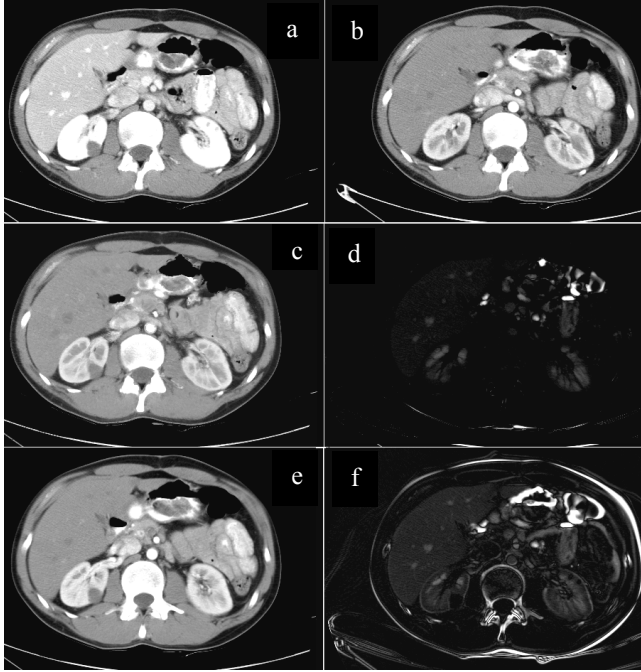


Figure 2: Intra-patient 3D registration. This example shows results of registering data from arterial and portal phase: (a) a 2D slice from portal phase; (b) the corresponding 2D slice at arterial phase, aligned by the position in the body, as seen at the spinal cord; (c) the registered image from (b) using the demons algorithm; (d) the difference image between (a) and (c) after non-rigid registration; (e) the registered image from (b) using affine registration (d) the difference image between (a) and (e) after affine registration; (f) the difference image between (a) and (e) after affine registration.

Unsurprisingly, non-rigid registration gives better alignment at organ level. The largest objects in the 3D volumes, in this case the liver, govern both rigid and affine registrations and introduce biases in the other abdominal regions. A smoother interpolation using cubic B-splines supports the non-rigid deformations better than an intensity preserving nearest neighbor interpolation. Registration results are validated by difference images between intra-patient registered data from multiple phases, which reflect the superior results of non-rigid registration.

Figure 2 illustrates an example of intra-patient registration of data from arterial and portal phase. Although the affine transform gives satisfactory results, the deformation is governed by the liver; note the improved alignment at the level of the left kidney and spinal cord using a non-rigid transform.

We noted empirically that the spleen and kidneys could be segmented correctly by 3D heterogeneous erosion in the portal phase. However, the liver requires a minimum of two phases (arterial and portal) for segmentation. The 4D

convolution is implemented to detect the four organs simultaneously.

The segmentation of the four organs (liver, spleen, left kidney and right kidney) is validated by overlaying the labeled data on the CT volumes. Each organ is correctly detected, as confirmed by experienced radiologists, and the segmentation results are robust throughout the database. Errors in estimation at the top and bottom slices of each organ are mainly due to low spatial resolution (5mm slice thickness). In a third of all cases, small areas of the heart muscle are labeled as liver. The main sources of errors are in the vena cava, only partly enhanced in the arterial and portal phases. Segmentation results in the axial plane are presented in Figure 3 and three dimensional renderings of the segmented data are shown in Figure 4.

The use of fixed-delays during image acquisition was a further cause of enhancement variability in individual organs, especially during the arterial phase acquisition. Automatic bolus tracking would be more appropriate for our application. Furthermore, the presence of abdominal abnormalities in our database adds aberrant values to the organ 3D intensity model. This database was used due to the unavailability of contrast-enhanced CT data of normal controls.

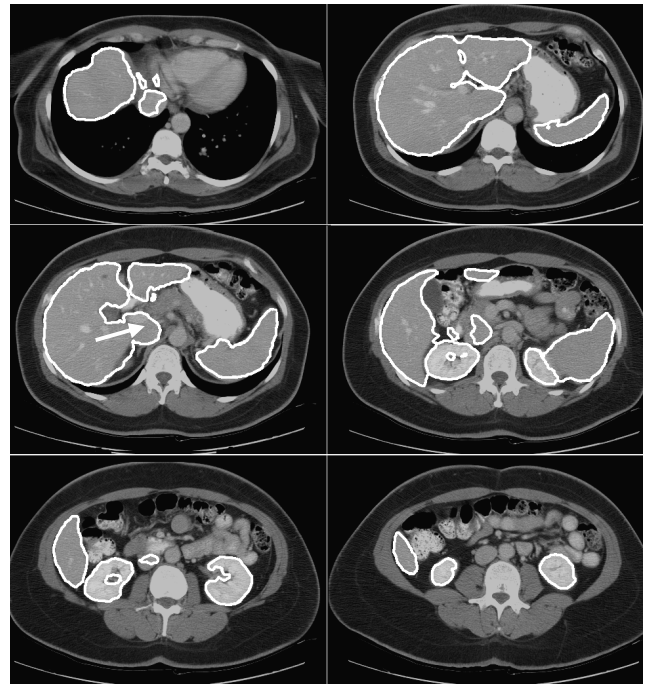


Figure 3: Segmentation results. The segmentation of liver, spleen and kidneys using the proposed algorithm are shown using white contours on CT data. We show 2D slices along the 3D CT volume from left to right and top to bottom. While the segmentation of four organs is reliable, the largest error appears in the vena cava, which is assimilated into the liver, as indicated by the arrow.

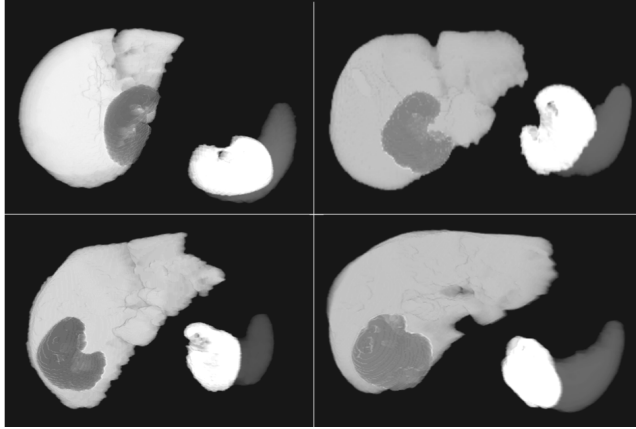


Figure 4: Multi-organ 3D volume rendering of four patients. The liver, spleen, right kidney and left kidney are presented as segmented by the proposed automatic algorithm.

5. DISCUSSION

Medical imaging and computer-aided diagnosis traditionally focus on organ- or disease-based applications. Very little work has been presented toward the automatic simultaneous detection and segmentation of multiple organs or different types of abnormalities. A multi-organ approach uses information on inter-organ boundaries and relative position, as well as permits a more comprehensive analysis toward methods for full abdominal computer-aided radiology (CAR) and diagnosis (CAD).

A fully automatic method is presented for the simultaneous segmentation of four abdominal organs from sixteen 4D CT data using heterogeneous erosion and level sets. Intra-patient data is registered using a non-rigid transformation and organ areas segmented by 4D convolution. This first segmentation is input into a refining geodesic active contour. Data from two CT phases contribute to the robust labeling of liver, spleen, and left and right kidney.

The automatic method employs a 3D intensity model; no a priori probabilistic on shape or location is used. We also exploit fewer CT phases than alternative work and propose a 4D convolution to detect targeted objects in the estimated range of intensities.

This 3D evaluation of abdominal data shows great promise as a clinical tool for multi-organ and multi-disease analysis. The future development of the study will allow building abdominal digital atlases, modeling abdominal variability, analyzing multi-organ patient data, monitoring treatment, interventions and disease development. Essentially, future work will focus on the development of multi-organ computer-aided radiology.

For immediate work, we will analyze images of higher resolution, normalized in intensity, and will include normal

controls for quantitative validation and correction of segmentation errors. Other abdominal organs (pancreas, stomach, gallbladder, etc.) will be simultaneously addressed.

ACKNOWLEDGEMENT

This work was supported by the Intramural Research Program of the National Institutes of Health, Clinical Center.

REFERENCES

- [1] V. Caselles, R. Kimmel and G. Sapiro, "Geodesic active contours", *International Journal on Computer Vision*, Vol. 22(1), pp. 61–97, 1997.
- [2] L. Gao, D.G. Heath and E.K. Fishman, "Abdominal image segmentation using three-dimensional deformable models" *Invest. Radiol.* Vol.33(6), pp. 348-355, 1998.
- [3] X. Hu, A. Shimizu, H. Kobatake and S. Nawano, "Independent analysis of four-phase abdominal CT images", Proceedings of MICCAI 2004, LNCS 3217, pp. 916-924, 2004.
- [4] D. Mattes, D. R. Haynor, H. Vesselle, T. K. Lewellen and W. Eubank, "PET-CT image registration in the chest using free-form deformations", *IEEE Trans. on Medical Imaging*, Vol. 22(1), pp. 120–128, 2003.
- [5] H. Park, P.H. Bland and C.R. Meyer, "Construction of an abdominal probabilistic atlas and its application in segmentation" *IEEE Trans. Med. Imaging* Vol. 22(4), pp. 483-492, 2003
- [6] P. Perona and J. Malik, "Scale-space and edge detection using anisotropic diffusion", *IEEE Trans. on Pattern Analysis and Machine Intelligence*, Vol. 12, pp. 629–639, 1990.
- [7] M. Sakashita, T. Kitasaka, K. Mori, Y. Suenaga and S. Nawano, "A method for extracting multi-organ from four-phase contrasted CT images based on CT value distribution estimation using EM-algorithm", Proceedings of SPIE Vol. 6509 , pp. 1C-1-12, 2007.
- [8] J.A. Sethian, "*Level Set Methods and Fast Marching Methods*", Cambridge University Press, 1996.
- [9] A. Shimizu, R. Ohno, T. Ikegami and H. Kobatake, "Multi-organ segmentation in three-dimensional abdominal CT images", *Int J CARS*, Vol. 1, pp. 76-78, 2006.
- [10] J.P. Thirion, "Image matching as a diffusion process: an analogy with maxwell's demons", *Medical Image Analysis*, Vol. 2(3), pp. 243–260, 1998.
- [11] C. Yao, T. Wada, A. Shimizu, H. Kobatake and S. Nawano, "Simultaneous location detection of multi-organ by atlas-guided eigen-organ method in volumetric medical images", *Int J CARS*, Vol. 1, pp. 42-45, 2006.